Hildebrand and Hansen Solubility Parameters from Molecular Dynamics with Applications to Electronic Nose Polymer Sensors

M. BELMARES,[1] M. BLANCO,[1] W. A. GODDARD, III,[1] R. B. ROSS,[2] G. CALDWELL,[2]
S.-H. CHOU,[2] J. PHAM,[2,*] P. M. OLOFSON,[2] CRISTINA THOMAS[2]
[1]*Materials and Process Simulation Center, California Institute of Technology, Pasadena, California 91125*
[2]*3M Company, St. Paul, Minnesota 55144-1000*

Received 17 September 2003; Accepted 4 June 2004
DOI 10.1002/jcc.20098
Published online in Wiley InterScience (www.interscience.wiley.com).

Abstract: We introduce the Cohesive Energy Density (CED) method, a multiple sampling Molecular Dynamics computer simulation procedure that may offer higher consistency in the estimation of Hildebrand and Hansen solubility parameters. The use of a multiple sampling technique, combined with a simple but consistent molecular force field and quantum mechanically determined atomic charges, allows for the precise determination of solubility parameters in a systematic way ($\sigma = 0.4$ hildebrands). The CED method yields first-principles Hildebrand parameter predictions in good agreement with experiment [root-mean-square (rms) = 1.1 hildebrands]. We apply the CED method to model the Caltech electronic nose, an array of 20 polymer sensors. Sensors are built with conducting leads connected through thin-film polymers loaded with carbon black. Odorant detection relies on a change in electric resistivity of the polymer film as function of the amount of swelling caused by the odorant compound. The amount of swelling depends upon the chemical composition of the polymer and the odorant molecule. The pattern is unique, and unambiguously identifies the compound. Experimentally determined changes in relative resistivity of seven polymer sensors upon exposure to 24 solvent vapors were modeled with the CED estimated Hansen solubility components. Predictions of polymer sensor responses result in Pearson R^2 coefficients between 0.82 and 0.99.

 J Comput Chem 25: 1814–1826, 2004

Key words: cohesive energy; Hansen solubility parameters; molecular dynamics method; electronic nose

Introduction

Chemicals such as trade-sales coatings, pharmaceuticals, cosmetics, and foodstuffs are produced as multicomponent chemical mixtures. Often these mixtures or formulations include polymers and low molecular components of high and low boiling points. Basic knowledge of the miscibility of the various components is required to meet environmental, shelf life, and product quality specifications. In this regard, Hildebrand and Hansen solubility parameters have played an important role in the development of stable commercial chemical formulations as well as for assessing phase segregation during product synthesis. However, the various experimental techniques to measure Hildebrand and Hansen solubility parameters lead to large uncertainties, and add inconsistencies across material property databases. This limits the practical use of solubility parameters. It can be argued that first principles predictions of Hildebrand solubility parameters should be of great practical value in chemical formulation work.

In 1936, Joel H. Hildebrand proposed[1] a simple definition for a "solubility parameter" that would provide a systemic description of the miscibility behavior of solvents. This solubility parameter δ is defined as the square root of the cohesive energy density, the heat of vaporization divided by the molar volume. Hansen[2] proposed an extension of the Hildebrand parameter method to estimate the relative miscibility of polar and hydrogen bonding systems. In Hansen's approach the Hildebrand solubility parameter is split into three components: polar, dispersion, and hydrogen bonding; thus, the name 3D solubility parameters. The three components are empirically adjusted to define the miscibility characteristics of the solvent. Solvents with similar Hansen solubilities are

**Current address:* University of St. Thomas, St. Paul, MN 55105
Correspondence to: W.A. Goddard; e-mail: wag@wag.caltech.edu
Contract/grant sponsors: ARO/MURI, 3M Company, and Owens Corning

miscible in most proportions; dissimilar values yield limited solubilities. Hildebrand and Hansen solubility parameters are useful for selecting solvents and additives in formulations, for the blending of polymers, for the control of kinetics and monomer sequence distributions in copolymers, and for the proper selection of time-release formulations in the delivery of pharmaceuticals.

A closely related problem is the prediction of changes in swelling of polymers in the presence of volatile organic compounds. The amount of swelling can be measured by changes in electrical conductivity. In this type of sensor, no individual detector is highly selective toward an individual analyte, as would be the case in the traditional "lock and key" approach to biochemical sensing. Instead, each detector responds to many analytes, and each analyte elicits a response from many detectors. The resulting odor signature from the array of broadly crossresponsive detectors is used to classify, and in some cases quantify, the analyte of concern. Vapor detectors based on this experimental principles have been used to produce an "electronic nose"[3] by Caltech scientists. A theoretical method to model the effect of "analytes" *a priori* on specific polymer sensors could further aid development of these devices.

General computational tools to estimate Hildebrand and Hansen solubility parameters have appeared in the literature. Choi and Kavasallis first used atomistic simulations to estimate the solubility parameters of a class of alkyl phenol ethoxylates,[4] and later applied it to the estimation of 3D Hansen solubility parameters.[5] A related method has been applied to the estimation of the solubility parameters for distributions of asphaltenes, resins, and oils from crude oils and related materials.[6] The accuracy of these methods depends on the correct building of the bulk structure as well as on the molecular force field parameters used in the calculations. Numerous approaches for building amorphous polymers and liquids have been published.[7–12] Some of these methods involve growing the polymer chains at a fixed experimental density using rotational isomeric state (RIS) statistics in combination with a scaled down atomic radius followed by potential energy minimization with periodic boundary conditions. Other methods simulate a "polymerization" process to grow the chain at a fixed density. A computationally expensive protocol involving chain growth at low density followed by a pressure-induced compression with molecular dynamics has also been reported.[13] Most of these methods have been successfully used to generate amorphous structures, and have correctly predicted the solubility parameters of a few polymers.

Here, we report on a multisample molecular dynamics method, which provides a feasible tool for estimating Hildebrand and Hansen solubility parameters *without* the need for experimental data. The molecular dynamics method developed in this work is particularly useful in rapidly generating structures of polymers with large monomer units containing rings or other complex groups. The finite number of densification and equilibration steps, regardless of polymer size, allows for a gradual packing adjustment and the uniform redistribution of stresses among the polymer chains. This new method was validated by several studies where solubility parameter calculations were successfully correlated with experimental measurements.

For improved accuracy, the new method employs quantum mechanical charges of single molecules. However, semiempirical methods for charge assignment, such as *Q*eq,[14] give somewhat comparable results for molecules containing first group elements. The most significant approximation comes from the use of a generic force field for the estimation of dispersion and hydrogen bonding contributions. Approximations not withstanding, calculated Hildebrand parameters compare well with experimental values for a series of solvents and monomer molecules. As an example of an application we illustrate the use of these calculated values to aid the selection of polymeric sensors for the Caltech electronic nose.

Methodology

The Hildebrand solubility parameter for a pure liquid substance is defined as the square root of the cohesive energy density.

$$\delta = [(\Delta H_v - RT)/V_m]^{1/2} \tag{1}$$

where Δ_v is the heat of vaporization, and V_m the molar volume. RT is the ideal gas pV term, and it is subtracted form the heat of vaporization to obtain an energy of vaporization. Typical units are

$$1 \text{ hildebrand} = 1 \text{ cal}^{1/2}\,\text{cm}^{-3/2} = 0.48888 \times \text{MPa}^{1/2}$$
$$= 2.4542 \times 10^{-2}\,(\text{kcal/mol})^{1/2}\,\text{A}^{-3/2}$$

Hansen[2] proposed an extension of the Hildebrand parameter to estimate the relative miscibility of polar and hydrogen bonding systems

$$\delta^2 = \delta_d^2 + \delta_p^2 + \delta_h^2 \tag{2}$$

where δ_d, δ_p, and δ_h are the dispersion, electrostatic, and hydrogen bond components of δ, respectively. For molecules whose heats of vaporization can be measured, or calculated, one can easily determine the value of δ. The Hansen solubility parameters in eq. (2) are determined empirically based on multiple experimental solubility observations. However, for polymers the Hansen parameters are assigned to the parameters of the solvent causing the maximum swelling in a series of polymer swelling experiments. Thus, the two quantities represented by eqs. (1) and (2) are expected to be similar but not identical, because the Hildebrand parameters are not always determined from heats of vaporization, particularly for substances with high boiling points. For polymers, a variety of other experimental methods are also employed[15] leading to a wide range of experimentally reported values.

NPT Molecular Dynamics Method

The Hildebrand solubility parameters, that is, heats of vaporization and densities, can be, in principle, calculated by running molecular dynamics at constant pressure and temperature for a cell under periodic boundary conditions. We illustrate this method by calculating the heat of vaporization and solubility parameter of ethylchloride using a generic force field, the Dreiding force field,[16] and quantum mechanically determined electrostatic potential atomic

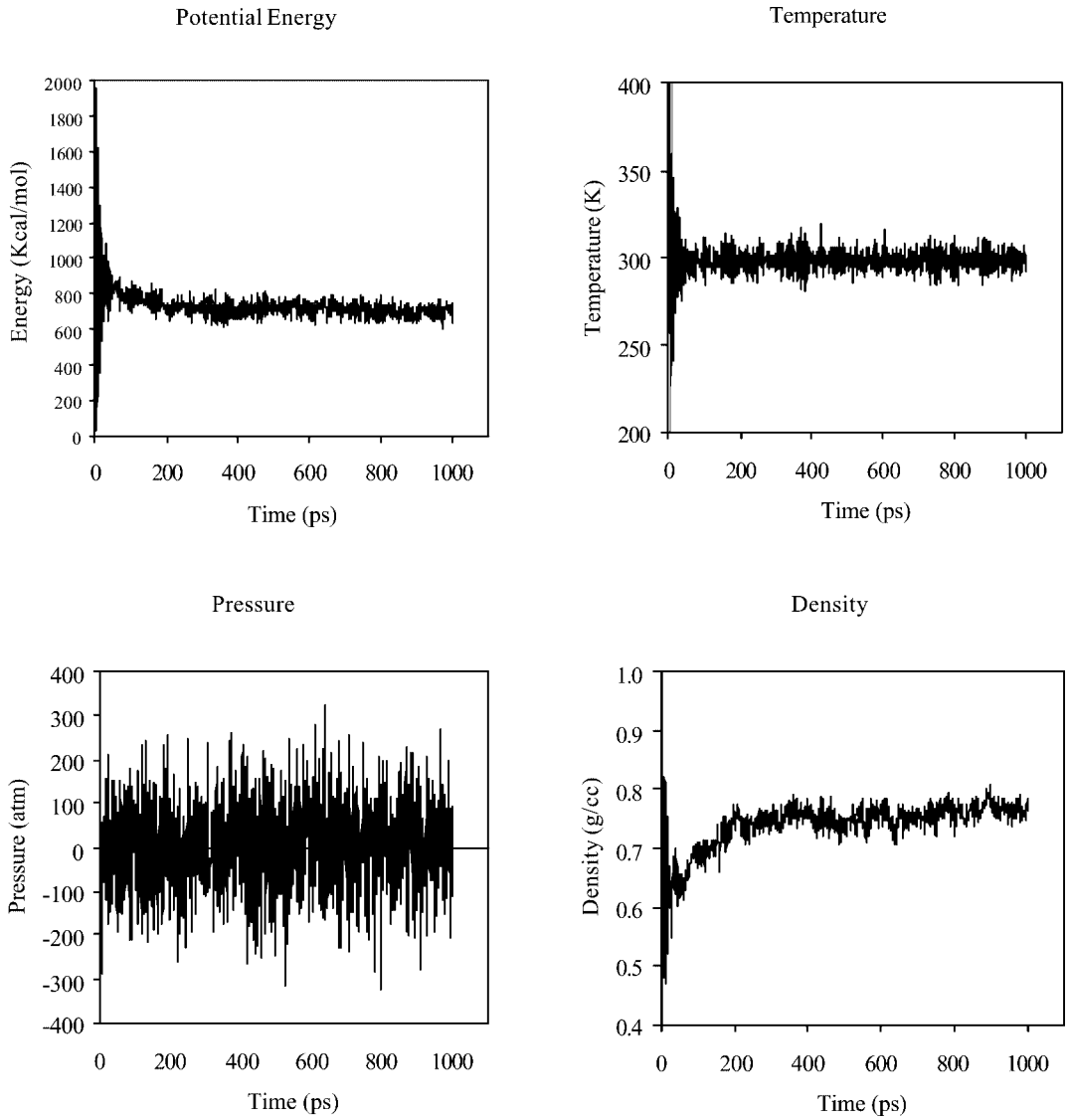

Figure 1. NPT Molecular Dynamics statistics on liquid ethylchloride. Initial density was set to the experimental value (0.92 g/cc). A Nose–Hoover thermostat was used to keep the temperature at 300 K. Pressure fluctuations are typical of liquid simulations using a Nose–Hoover barostat. The density is still climbing after an initial drop due to a volume expansion caused by the initial random velocity distribution. After 1000 ps the density has not yet reached equilibrium.

charges $[C(-0.049)H_3(0.0424)C(-0.077)H_2(0.1079)Cl(-0.217)$ numbers in parenthesis are in electron charge units]. For simplicity we start the simulation using the experimental liquid density (0.9 g/cc), a requirement that becomes unnecessary in the method described as the Cohesive Energy Density (CED) protocol below. We prepared a sample containing 256 ethylchloride molecules using the Amorphous Builder in Cerius2.[17] After 200 ps of thermal equilibration we ran the simulation an additional 800 ps for a total time of 1 ns, a single NPT Nose–Hoover molecular dynamics run. Potential energy, temperature, pressure, and density are given as a function of time in Figure 1.

We observe that the final density (0.76 g/cc) falls 16% short of the experimental value (0.90 g/cc) even though the initial density was used to start the simulation. The calculated heat of vaporization is 15% too low.ΔH_{vap} is calculated from the energy of periodic unit cell minus the sum of the individual molecules E_i averaged over the P time samples.

$$\Delta H_{vap} = \left\langle E_{cell} - \sum_{i=1}^{n} E_i \right\rangle_P + RT \tag{3}$$

Table 1. Sampling Effects on the Liquid Properties of Ethylchloride Using the NPT Method.

Sample size P	CED cal/cc[a]	Sdev cal/cc	UC vol A**3	Sdev A**3	Density g/cc	Sdev g/cc	ΔH_{vap} kcal/mol[b]	SP (δ) (cal/cc)$^{1/2}$[c]
2	51.66	1.48	36042	219	0.76	0.009	4.98	7.19
4	52.12	1.36	35978	209	0.76	0.009	5.02	7.22
6	52.25	1.69	35978	329	0.76	0.010	5.03	7.23
8	51.96	1.35	36053	353	0.76	0.011	5.00	7.21
10	50.95	1.44	36436	610	0.75	0.013	4.98	7.14
25	51.70	1.85	36221	618	0.76	0.011	4.98	7.19
50	51.48	1.68	36300	600	0.76	0.012	4.96	7.17
100	51.29	2.00	36369	713	0.75	0.015	5.00	7.16
160	51.17	1.74	36384	610	0.75	0.016	4.99	7.15
250	51.33	1.64	36342	593	0.75	0.012	5.01	7.16
400	51.25	1.86	36364	665	0.75	0.011	5.00	7.16

[a]CED = cohesive energy density, UC Vol = unit cell volume, Hvap = heat of vaporization.
[b]Experimental heat of vaporization is 5.89 kcal/mol at 285.42 K, P = 101.325 kPa (ref. 30).
[c]Experimental solubility parameter (SP) is 9.2 (cal/cc)$^{1/2}$.

Figure 1 shows that the density is still steadily increasing after 1-ns simulation, and it may reach a good value given enough time. This is typical of large samples (hundreds of molecules) where random velocities are initially assigned to a potential energy minimized sample. The initial random nature of the assigned Boltzmann velocities causes an initial expansion on the sample. As time evolves, the intermolecular interactions bring the sample back towards higher densities. Sampling size effects on the liquid properties of ethylchloride are given in Table 1. In each case P samples were taken at equal time intervals from the last 800 ps. Note that no significant changes in liquid properties are observed after P = 10 samples. Consequently, in a protocol described below we focused on (a) smaller samples (16–64 molecules), (b) multiple, independent, and short molecular dynamics runs, (c) a process of contractions and expansions to accelerate density convergence.

CED Method

We report here the CED method to determine an ensemble of temperature and pressure equilibrated structures from which we can extract condensed phase properties, including the Hansen and Hildebrand solubilities of solvents and polymers. CED leads to sample standard deviations in these quantities, within the model and size limitations of the ensemble that are often lower than the experimentally measured deviations.

The CED method overcomes the common equilibration problems with condensed phase molecular dynamics, that is, how to choose initial molecular configurations not far from equilibrium at normal densities. Significant amounts of simulation time are usually required to equilibrate the initially random packed molecules often generated with Monte Carlo methods. In particular, densely packed simulated polymers often lead to highly nonequilibrated dihedral populations. Thus, care must be taken to generate an ensemble of thermally accessible conformations not far from equilibrium. These two requirements, condensed phase densities and equilibrated molecular conformations, are satisfied through the following method:

1. A cubic periodic unit cell containing a given number of molecules is built at a low density, $_{low}$, typically 50% of the target density. Generally four polymer chains are sufficient, although for very high molecular weights even one chain can be adequate. For solvents 16 to 64 solvent molecules are adequate. We find that for packing the structure, it is useful to scale van der Waals radii by a factor of 0.30 to get initial structures that will eventually lead to a good ensemble. In cases where the compounds are polymers, or a molecule with a large number of torsional degrees of freedom, we use the Amorphous Builder in Cerius2[17] to create the initial low-density sample. The initial polymer amorphous structures are constructed using the rotational isomeric state (RIS) table and a suitable Monte Carlo procedure to achieve a correct distribution of conformational states in the low-density sample. The Amorphous Builder converts an existing model into an amorphous structure by manipulating the model's rotatable bonds. Each unique torsion can be defined using a Monte Carlo procedure, with statistical weights given by a previously built rotational isomeric state table determined with well established molecular mechanics dihedral sampling procedures. Conformations are rejected if two or more atoms come closer than a van der Waals scale distance. In polymer calculations, the number of monomers in each chain is usually determined such that the total volume of the four chains is at least 6000 Å.^{3} Alternatively, a degree of polymerization of 30 suffices to give values comparable to experiment. In such polymer samples, the minimum number of atoms is at least 1000. Larger samples are recommended whenever possible.
2. For convenience, we used the experimental density of the solvents and polymers as a target value because these were available in the literature. For liquid systems with unknown densities we typically run a preliminary CED calculation with

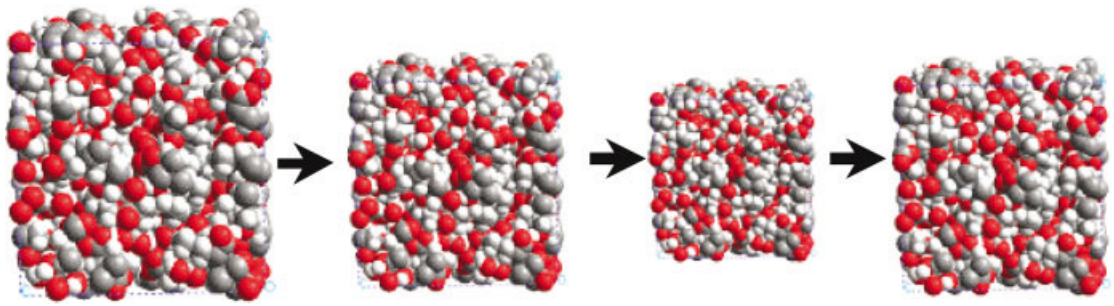

Figure 2. A polymer or solvent sample is put through a series of compression and expansion steps until the proper density and packing is obtained. On the left, the initial density is 0.4 ρ_o, 40% of the target density. After compression, the second step, the sample is over compressed to 1.2 ρ_o. Finally, the sample is allowed to relax. Through NPT molecular dynamics a final prediction of the density and cohesive energy of the sample is obtained. The process is repeated for a few samples to gather statistics.

a rough "trial" density, such as that predicted from group additivity methods, to obtain a good initial estimate (see Fig. 5). The procedure below will increase the density to a maximum, ρ_{high}, typically 125% of the target density. The resulting amorphous structure is then relaxed, resulting in a predicted target density for the start of the definitive CED calculation.

3. The charges of the isolated solvent or polymer molecules are defined using the charge equilibration method[14] or are obtained from quantum mechanical calculations (ESP or Mulliken charges).
4. The force field parameters are taken from a suitable force field, such as the generic Dreiding force field,[16] Universal force field (UFF[18]) etc.
5. Minimization: the potential energy of the bulk system is minimized for M steps, typically 5000 steps, or until the atom rms force converges to 0.10 kcal/mol-Å whichever comes first.
6. Annealing dynamics to allow the structures to equilibrate typically 750 steps of Molecular Dynamics (1 fs/step) at high temperature (typically between 400 and 800 K, with 700 K generally adequate) using canonical fixed volume dynamics (NVT) are carried out to anneal the sample.
7. Compression: the reduced cell coordinates are shrunk such that the density is increased by $(\rho_{high} - \rho_{low})/N$, where N is typically 5.
8. The atomic coordinates are minimized, and dynamics run on the system with the previously described procedure holding the cell fixed (steps 5–6).
9. A total of N compression, minimization, and dynamics cycles are performed until the density reaches ρ_{high} , typically 125% of the target density, steps 5–8.
10. The cell parameters are then increased in N cycles of expansion, minimization, and dynamics, until the target density is reached.
11. The sample is allowed to relax in M steps of minimization allowing both the cell and the atomic coordinates to relax.
12. Molecular dynamics are performed for a time to thermalize and then to measure properties. Typically, we do as few as 20 ps, but longer times are recommended for high molecular weight compounds. The first 10 ps are used for thermalization of the sample at the desired temperature. The last 10 ps are used for averaging of cell volume and potential energy components: van der Waals (dispersion), electrostatic (polar), and hydrogen bonding.
13. The Hansen enthalpy components are calculated by subtracting the potential energy of the bulk system from the sum of the potential energies of the individual molecules in vacuum.
14. This process is repeated P times, with different initial random conformations and packing. Typically $P = 10$ is adequate, but higher values are recommended.
15. Hansen solubility parameters and molar volumes are computed as well as their standard deviations. We use the 95% confidence limit of an F statistical distribution test, two standard deviations from the average value, to identify outliers.[19] Typically a $P = 10$ sample run will have no outliers; more than two outliers are rare.

The overall procedure is schematically illustrated in Figure 2.

Hildebrand and Hansen solubilities are calculated from the molecular dynamics average potential energy components of the condensed phase simulation, single unit cell E_c^k, the energy components of the individual molecules, E_i^k, and the volume of the simulated sample, V_c as follows

$$\delta_k^2 = \left(\frac{\sum_{i=1}^{n} \langle E_i^k - E_c^k \rangle}{N_o \langle V_c / n \rangle} \right) \tag{4}$$

where $\langle\rangle$ indicates a time average over the duration of the dynamics, n the number of molecules, $k = 1,2,3$ for coulomb (polar), van der Waals (dispersion) and hydrogen bond components, $E_{\text{H-bond}}$, E_{coulomb}, $E_{\text{dispersion}}$, respectively, and N_o is Avogadro's number. Because we use the total potential energy, instead of enthalpy, it is not necessary to subtract the ideal gas pV term. For the same reason, the sum of the square of the three Hansen components [right-hand side of eq. (2)] may differ from δ,^{2} the total Hildebrand solubility parameter, as calculated through eq. (1). Such is the case because δ^2 also contains averages over valence terms, while the Hansen components include only nonbond interactions. The average difference between the Hildebrand solubility parameter and

the sum of the Hansen components is 0.09 hildebrands, and the largest deviation is 0.3 hildebrands. We stress the importance of using the thermally equilibrated ensemble of molecular conformations to estimate the gas phase terms E_i^k, instead of n times the minimized energy of one molecule. For the gas phase terms we use the gas phase ensemble average of the isolated molecules taken directly from the condensed phase simulation, averaged over the entire molecular dynamics at the desired temperature.

Results

Sixty-four common solvents, reactants, and monomers of significantly different structure, polarity, and chemical composition were chosen from various experimental compilations of Hildebrand solubility values available in the literature. To obtain consistent charges for all molecules, we minimized the structure with Quantum Mechanics (Hartree–Fock 6-31G** full geometry optimization) and then evaluated both the Mulliken and the ESP charges (fitted to the electrostatic potential with a constraint to reproduce the quantum dipole moment from the wave function). These systematic choices allow predictions on a variety of solvents without the need to use experimental data. We carried out independent simulations with both sets of charges.

Table 2 contains the Hildebrand solubilities and densities averaged over $P = 10$ CED simulations for the two charge assignment methods for each of the 64 solvent/monomer compounds. For comparison, the various experimental values found in the literature and their deviations are included. Table 3 contains the calculated Hansen solubilities. Because the experimental Hansen solubilities are fitted to reproduce the miscibility characteristics of mixed solvents, no direct comparison with the formal theoretical definition based on eq. (2) is possible. For example, experimental hydrogen bond Hansen parameters are nonzero, even for solvents that lack hydrogen bond donors, such as ketones. Table 4 gives an example of the output file obtained with our current software implementation of the CED procedure described above.

Figures 3 and 4 show linear correlations between experimental and predicted values. The average experimental standard deviations of the Mulliken and ESP CED methods and the various literature sources are 0.38 and 0.45, and 0.39 hildebrands, respectively. Although most solvents fall within the experimental error, a few predictions are clearly outside the range of measured values. The CED method rms deviation when compared with averaged experimental values is 1.17 and 1.59 hildebrands for the ESP and Mulliken CED methods, respectively. Exclusion of the six worst cases (formic acid, acetic acid, dichlorodifluoromethane, acrylic acid, methyl formamide, and malononitrile) from the predictions reduces the calculated vs. experimental rms deviation to 0.7 and 1.35 hildebrands for the CED method with ESP and Mulliken charges, respectively. Figure 5 shows the predicted vs. experimental densities. The root-mean-square error between model and experiment is 0.05 g/cc for both charge assignment methods. The accuracy of the molecular dynamics results directly depends on the accuracy of the intra- and intermolecular potential atomic parameters (force field) and to some extent on the modeling protocol. This problem is, in part, overcome with force fields that accurately reproduce the experimentally measured bond distance, angles, and the respective force constants of small molecules. Less effort has gone into optimizing the van der Waals parameters in such force fields. Precision, on the other hand, is strongly dependent on the molecular dynamics procedure employed to prepare the samples. No significant differences in precision were found for the worst 10 cases (between 0.25 to 0.71 hildebrands standard deviation) when compared to the average precision across all solvents (0.44 hildebrands).

We speculate that the assigned van der Waals force field parameters (our generic force field was not particularly fitted to halogens and nitrogen containing compounds) play a role in the accuracy of our predictions. We made no attempt to adjust the force field parameters here. However, we point to the possibility of using the CED method together with experimental heats of vaporization and densities for the estimation of van der Waals parameters and/or the hydrogen bond terms for the various chemical atom types represented by these compounds. For example, systematic underestimation of the solubility parameter is observed through the calculated vs. experimental ratio $\delta_{esp}/\delta_{exp}$ for alcohols and amides (2-ethyl-1hexanol 0.89, 2-ethyl-1-butanol 0.92, 1-pentanol 0.95, *n*-butanol 0.92, *n*-propanol 0.91, furfuryl alcohol 0.96, ethanol 0.87, 1,3-butanediol 0.91, methanol 0.89, *N,N*-dimethylacrylamide 0.91, dimethylacetamide 0.94, dimethylformamide 0.87, methylformamide 0.84). This suggests that the Dreiding parameters for the H-bond term (Do = 4.0 kcal/mol, Ro = 2.75 Å) could be modified to increase the accuracy of the predictions. Both parameters may be involved because the density of these two groups of compounds is also underestimated. Finally, there seems to be a systematic overestimation of the solubility parameter for the organic acids. The $\delta_{esp}/\delta_{exp}$ ratio is consistently high (propionic acid 1.18, acetic acid 1.30, methacrylic acid 1.04, formic acid 1.30, acrylic acid 1.21). The effect is opposite the hydrogen bond effect previously mentioned. We assume that the molecules in the gas phase are noninteracting. Many low molecular weight acids exist in a dimerized form in the gas phase. If we assume that half of the intermolecular hydrogen bonds are preserved in the gas phase, the solubility parameter will be decreased by about 3 hildebrands, bringing theory and experiment to closer agreement. We now discuss the effect of charge assignment methods.

Although Mulliken charges are quite useful in determining the structure of molecules in the gas phase, these appear to be less accurate than Electrostatic Potential charges (ESP) for the determination of condensed phase properties. It appears that the far field representation of the ESP charges captures more accurately the physical interactions between molecules in the condensed phase. However, we caution the user to the high sensitivity of ESP charges to the choice of quantum mechanical basis sets. We cautiously advocate the use of ESP charges for the estimation of solubility parameters and the use of Mulliken charges for conformational studies in the gas phase.

We compare our Molecular Dynamics results to other predictive methods available in commercial software packages such as Synthia–Fedors and Synthia–van Krevelen.[20] These methods can be considered state-of-the-art group additivity methods, relying on topological descriptors and other single molecule quantities to make predictions based on correlations and parameter extractions from large databases of solubility parameters. Although intended for predictions on polymers, these parametric methods have been

Table 2. Comparison of Calculated and Experimental Solubility Parameters and Condensed Phase Densities at Room Temperature for 64 Common Solvents, Reactants, and Monomers.

Compound	MUL δ[a]	Std. dev.	ESP δ[b]	Std. dev.	Exptl. δ[c]	Std. dev.	Exp.[18]	Exp.[19]	Exp.[20]	Exp.[21]	Exp.[22]	Exp.[23]	Exp.[24]	Mulliken density	ESP density	Exp. density[d]
1,3-Butadiene	7.32	0.38	7.33	0.68	7.10	0.39	7.77	7.1	7.1					0.64	0.65	0.62
1,3-Butanediol	12.67	0.33	12.8	0.52	14.14	1.59	13.76	11.6	10.9	—	—		14.14	0.94	0.91	1.01
1,4 Dioxane	13.2	0.24	10.3	0.5	9.02	1.58	10.13	7.9						1.06	0.99	1.03
1-Chlorobutane	8.19	0.2	8.78	0.32	8.44	—		—	—	—	—		8.44	0.86	0.87	0.89
1-Pentanol	9.51	0.18	10.1	0.48	10.60	0.47	11.12	—	11.6	—	—	10.63	10.60	0.76	0.75	0.81
2-Ethyl-1-butanol	9.15	0.46	9.52	0.35	10.38	0.74	—	10.5	11.9	—	—	10.39	10.38	0.77	0.78	0.83
2-Ethyl-1-hexanol	8.97	0.54	8.75	0.45	9.85	0.33	10.15		9.5	—	—		9.85	0.78	0.76	0.83
2-Ethylhexyl acrylate	8.99	0.32	8.58	0.44	8.64	0.05	7.87	7.8	—	—		—	—	0.84	0.85	0.89
Acetic acid	12.88	0.66	13.5	0.62	10.35	1.31	13.01	10.2	10.1	—	12.6	10.49	10.35	1.03	1.04	1.05
Acetone	10.79	0.5	10.2	0.59	9.77	0.15	9.62	9.9	—	10	10	9.80	9.77	0.82	0.82	0.79
Acetonitrile	12.49	0.55	11.6	0.49	11.92	0.11	12.11	11.9	11.9	11.9	11.9	11.96	11.75	0.8	0.80	0.79
Acrylic acid	14.49	0.28	15	0.37	12.30	0.51	12.89	12	12	—	—	—	—	1.06	1.04	1.05
Benzene	10.34	0.47	9.84	0.51	9.15	0.03	9.16	9.2	9.2	9.2	9.15	9.11	9.15	0.92	0.93	0.88
Carbon tetrachloride	9.64	0.45	9.32	0.29	8.65	0.05	8.55	8.6	8.6	8.6	8.6	8.72	8.65	1.67	1.63	1.59
Chlorobenzene	10.32	0.39	10.5	0.5	9.57	0.07	9.67	9.5	—	9.5	9.5	9.60	9.57	1.1	1.13	1.11
Cyclohexane	8.44	0.33	8.59	0.37	8.18	0.42	8.19	8.2	9.3	8.2	8.2	8.23	8.18	0.76	0.78	0.78
Cyclohexanol	10.15	0.47	10.5	0.47	9.88	0.27	10.42	9.9	9.9	9.9	—	9.60	9.88	0.86	0.85	0.96
Cyclohexanone	10.35	0.44	9.87	0.38	10.16	0.37	10.42	9.9						0.94	0.92	0.95
Dichloro, difluoromethane	10.89	0.36	8.52	0.4	5.81	0.44		5.5				6.13		1.62	1.56	1.49[e]
Di-ethyl amine	7.61	0.33	8.66	0.58	7.96	0.03	8.04	8	—	—	—	7.99	7.96	0.65	0.71	0.71
Diethyl ether	8.92	0.4	7.45	0.57	7.62	0.16	—	7.4	—	7.4	7.4	7.74	7.62	0.75	0.69	0.71
Diethyl phthalate	11.3	0.38	10.2	0.47	9.55	0.05	9.97	10	—	—	10.05	10.09	—	1.08	1.05	1.12
Di-isobutyl-ketone	8.68	0.44	8.55	0.27	8.17	0.25	—	7.8	—	—	—	8.28	8.17	0.81	0.82	0.81
Dimethyl sulfoxide	14.71	0.34	15.6	0.57	14.50	—		14.5						1.11	1.15	1.10
Dimethylacetamide	11.13	0.39	10.1	0.42	10.80	—		10.8						0.91	0.88	0.94
Dimethylformamide	11.97	0.47	10.4	0.14	11.95	0.22	11.79	12.1						0.9	0.88	0.94
Di-propyl amine	7.42	0.5	8.42	0.2	7.79	0.10	7.97		—	—	—	7.79	7.79	0.67	0.70	0.74
Ethanol	11.75	0.64	11.2	0.51	12.92	0.12	12.78	12.7	—	12.8	12.7	12.99	12.92	0.76	0.72	0.79
Ethyl acrylate	11.22	0.71	10.4	0.32	8.60	0.21	8.81	8.6	—	—	8.4	—	—	0.93	0.92	0.92
Ethyl benzene	9.48	0.26	9.33	0.41	8.80	0.04	8.84	8.8	—	8.8	8.8	8.72	8.80	0.88	0.88	0.87
Ethyl chloride	8.21	0.54	8.23	0.7	8.85	0.49	—	9.2	—	—	8.5			0.88	0.89	0.90
Ethyl methacrylate	10.76	0.62	9.75	0.24	8.35	0.07	—	8.3	—	—	8.4	—	—	0.93	0.90	0.92
Ethylene carbonate	16.88	0.33	14.7	0.39	14.60	0.11	—	14.7	—	14.7	14.5	14.50	—	1.32	1.27	1.32
Formic-acid	15.6	0.51	15.8	0.59	12.15	1.28		12.1	14.7			12.20	12.15	1.2	1.16	1.22
Furfuryl alcohol	13.79	0.3	12	0.27	12.50	—		12.5						1.13	1.07	1.14
γ-Butyrolactone	14.57	0.33	12.6	0.31	12.74	0.19	12.87	12.6						1.12	1.10	1.13
Glycerol	16.51	0.82	15.6	0.32	15.50	3.63	17.69	16.5	9.9	16.5	16.5		21.1	1.14	1.09	1.26
Hexane	7.47	0.47	7.38	0.69	7.24	0.02	7.27	7.3	7.3	7.3	7.3	7.30	7.24	0.65	0.65	0.66
Maleic anhydride	17.18	0.5	14.8	0.28	13.60	—		13.6						1.42	1.38	1.31
Malononitrile	14.74	0.31	12.9	0.42	15.10	—		15.1						1.05	1.03	1.10
Methacrylic acid	10.94	0.48	11.6	0.45	11.20	1.10	13.11	11.2	11.2					0.96	0.97	1.02
Methanol	12.91	0.55	12.6	0.71	14.30	0.08	14.5	14.5	14.5		14.5	14.50	14.3	0.74	0.69	0.79
Methyl formamide	14.11	0.38	13.3	0.57	15.75	0.49		16.1	15.4					0.95	0.92	1.01
Methyl methacrylate	11.62	0.55	9.69	0.4	8.91	0.28	9.23	8.8	—	—	8.7		—	0.95	0.92	0.94
Methyl-ethyl-ketone	9.88	0.27	9.43	0.37	9.27	0.06	9.45	9.3	—	9.3	9.3	9.31	9.27	0.81	0.80	0.81
Methyl-isobutyl-ketone	9.68	0.3	9.12	0.38	8.57	0.12	—	8.4	—	—	—	8.33	8.57	0.83	0.83	0.80
N,*N*-Dimethylacrylamide	11.07	0.36	9.86	0.37	10.80	—	—	10.8	—	—	—	—	—	0.92	0.90	0.96
n-Butanol	9.89	0.56	10.4	0.46	11.30	0.84	11.6	11.4	13.6	11.4	11.4	11.32	11.30	0.75	0.75	0.81
n-Butyl acrylate	10.18	0.47	9.38	0.46	8.68	0.20	8.63	8.5	—	—	8.9	—	—	0.9	0.89	0.89
n-Butyl methacrylate	9.61	0.44	9.01	0.38	8.20	0.00	—	8.2	—	—	8.2	—	—	0.89	0.88	0.89
Neopentane	7.3	0.88	7.18	0.68	6.30	—		6.3						0.63	0.64	0.61
N-Methylpyrrolidinone	11.54	0.41	10.6	0.35	11.30	—	—	11.3	—	—	—	—	—	0.99	0.96	1.03
n-Propanol	10.28	0.43	10.9	0.6	11.97	0.57	12.18	11.9	10.5	11.9	11.9	12.01	11.97	0.72	0.71	0.80
o-Dichlorobenzene	10.56	0.2	10.3	0.25	9.98	0.03	10.04	10	—	—	—	10.05	9.98	1.3	1.31	1.30
Propiolactone	15.05	0.33	13	0.46	13.30	—		13.3						1.15	1.12	1.15
Propionic acid	11.73	0.25	12	0.49	10.16	2.20	12.47	9.9	8.1					0.96	0.94	0.99
Propionitrile	11.03	0.33	10.2	0.46	10.73	0.07	10.73	10.8	—	10.8	10.7	10.63	—	0.8	0.76	0.77
Propylene carbonate	14.64	0.41	13.1	0.48	13.33	0.04	—	13.3	—	—	—	13.38	13.3	1.18	1.16	1.19
Styrene	9.85	0.4	9.74	0.36	9.30	0.25	9.35	9.3	9.3	9.3	8.66	9.31	9.30	0.91	0.92	0.91
Succinic anhydride	16.76	0.46	15.2	0.4	15.40	—		15.4						1.32	1.32	1.23
Tetrahydrofuran	11.44	0.37	9.64	0.49	9.10	—		9.1						0.92	0.87	0.89
Tetrahydronaphthalene	9.89	0.41	9.75	0.31	9.60	0.17	9.5	9.5	—	—	—	9.80	—	0.95	0.94	0.97
Toluene	9.56	0.2	9.23	0.66	8.94	0.08	8.95	8.9	8.9	8.9	8.9	9.11	8.91	0.89	0.86	0.87
y-Butyrolactone	13.99	0.26	12.7	0.3	12.79	0.13	12.87	12.6	—	—	—	12.89	12.78	1.11	1.11	1.13
rms error	1.59		1.17											0.05	0.05	
Average standard dev.		0.38		0.45		0.39										

[a]Simulations employing Mulliken charges $(cal/cc)^{1/2}$.

[b]Simulations employing electrostatic potential charges $(cal/cc)^{1/2}$.

[c]Average of experimental values,[24,31–37] in $(cal/cc)^{1/2}$.

[d]Aldrich Catalogue, Sigma-Aldrich Co. Densities are in g/cc.

[e]Density at −29.7°C.

Table 3. Calculated Hansen Solubility Parameters for Some Common Solvents and Monomers vs. Charge Assignment Method.

	Mulliken $(cal/cc)^{1/2}$			ESP $(cal/cc)^{1/2}$		
Compound	δ_{elec}	δ_{disp}	δ_{hbond}	δ_{elec}	δ_{disp}	δ_{hbond}
1,3-Butadiene	0.94	7.31	0	1.63	7.45	0
2,Ethyl-1-butanol	4.13	7.63	2.59	4.94	7.53	3.19
2-EthylHexylacrylate	4.26	7.91	0	3.63	7.92	0
Acetone	6.98	8.23	0	6.2	8.11	0
Acetonitrile	10.06	7.51	0	8.79	7.54	0
Acrylic acid	10.52	8.45	5.15	11.33	8.08	5.22
Butyrolactone	10.98	9.47	0	8.39	9.44	0
Cyclohexanone	4.92	9.07	0	4.49	8.86	0
Dichlodifluoromethane	5.22	8.76	0	0.49	8.51	0
Diethyl phthalate	7.29	8.76	0	5.23	8.68	0
Diethylether	4.71	7.77	0	1.86	7.16	0
Diisobutylketone	3.43	7.92	0	2.93	7.96	0
Dimethylacetamide	7.52	8.54	0	5.55	8.34	0
Dimethylsulfoxide	11.39	9.31	0	12.48	9.38	0
1,4-Dioxane	9.59	9.01	0	4.89	9	0
Dipropylamine	1.14	7.36	0.73	3.48	7.49	1.9
dmf	8.81	8.11	0	6.71	8.14	0
Ethanol	7.57	7.31	4.89	7.65	6.71	4.94
Ethyl acrylate	7.45	8.33	0	5.77	8.55	0
Ethylchloride	2.71	7.68	0	3.55	7.67	0
Ethylenecarbonate	13.95	9.64	0	10.84	9.73	0
Ethylmethacrylate	6.68	8.46	0	4.77	8.3	0
Formic acid	11.62	7.83	6.32	12.45	7.2	6.55
Furfuryl alcohol	9.32	9.39	3.99	6.68	9.25	3.78
γ-Butyrolactone	10.36	9.42	0	8.46	9.53	0
Maleic anhydride	13.92	10.06	0	10.91	10.15	0
Malonitrile	12.31	8.22	0	9.95	8.39	0
Methyl-isobutylketone	4.96	8.24	0	4.11	8.26	0
Methanol	9.87	6.37	5.86	9.29	5.82	5.79
Methylmethacrylate	7.92	8.54	0	5.2	8.31	0
n-Butyl acrylate	6.01	8.35	0	4.72	8.3	0
n-Butylmethacrylate	5.08	8.25	0	3.87	8.19	0
Neopentane	0.74	7.16	0	1.43	7.34	0
N-Methylacetamide	8.55	7.94	4.12	8.25	7.82	4.27
N-Methyl *N*-vinylacetamide	7.03	8.63	0	5.32	8.51	0
N-Methyl Pyrrolidinone	7.34	9.15	0	5.68	8.95	0
N,*N* dimethylacrylamide	6.82	8.41	0	5.22	8.47	0
o-Dichlorobenzene	3.66	10.02	0	2.5	10.11	0
Propanoic acid	7.36	8.05	4.41	7.68	7.72	4.64
Propiolactone	11.91	9.23	0	9.18	9.23	0
Propionitrile	8.02	7.86	0	6.68	7.53	0
Propylenecarbonate	11.44	9.14	0	9.23	9.2	0
Styrene	3.15	9.6	0	2.49	9.39	0
Succinic anhydride	13.57	9.77	0	11.6	9.75	0
Tetrahydrofuran	6.67	9.16	0	3.5	8.87	0
Tetrahydro naphthalene	2.06	9.64	0	1.2	9.52	0
Toluene	2.7	9.2	0	1.76	9.16	0

used in practice to predict solubility parameters for solvents. The methods are fast and simple to use. In contrast, the MD method presented here requires a full-condensed phase simulation of the compound of interest. Nonetheless, the CED Molecular Dynamics method is nonparametric. Beyond the predetermined force field, in our case a generic force field[16] published in 1990, CED used no adjustable parameters and no experimental input information. Moreover, in principle, the CED molecular dynamics method can make predictions, as a function of pressure and temperature, and it is general enough to deal with complex mixtures, including sol-

Table 4. Example of Output from the CED Molecular Dynamics Method.

Sample	Cohesive energy (cal/cc)	Solubility parameter $(cal/cc)^{1/2}$	Density (g/cc)	End-end distance (A)	Radius gyration (A)	Hansen solubilities		
						Elec	Dispersion $(cal/cc)^{1/2}$	H-bond
1	−73.42	8.57	0.80	7.10	3.19	3.52	7.56	0.00
2	−81.04	9.00	0.88	6.78	3.19	4.05	8.31	0.00
3	−67.84	8.24	0.83	7.17	3.17	3.20	7.72	0.00
4	−77.06	8.78	0.83	7.63	3.26	3.60	7.84	0.00
5	−70.63	8.40	0.84	7.33	3.17	3.60	7.86	0.00
6	−70.46	8.39	0.82	6.67	3.22	3.18	7.72	0.00
7	−77.91	8.83	0.87	7.34	3.13	3.42	8.21	0.00
8	−81.90	9.05	0.87	7.17	3.19	4.00	8.15	0.00
9	−70.78	8.41	0.85	6.82	3.18	3.81	7.94	0.00
10	−65.89	8.12	0.82	6.74	3.19	3.96	7.87	0.00

	Average Standard deviation
Density	0.84±0.03 (g/cc)
Cohesive energy density	−73.69±5.52 (cal/cc)
Solubility parameter	$8.58\pm0.32\ (cal/cc)^{1/2}$
	$17.55\pm0.66\ (Mpa)^{1/2}$
Electrostatic Hansen SP	$3.63\pm0.32\ (cal/cc)^{1/2}$
Dispersion Hansen SP	$7.92\pm0.24\ (cal/cc)^{1/2}$
Hydrogen Bond Hansen SP	$0.00\pm0.00\ (cal/cc)^{1/2}$
Nonbond EEX	−76.05±5.49 (cal/cc)
Unit cell volume	$5820.43\pm174.32\ A^3$
End-to-end distance	7.07±0.3134 (A)
Radius of gyration	3.19±0.0334 (A)

Here the simulation procedure used 10 samples to estimate the condensed phase properties of 2-ethylhexylacrylate.

vent/polymer mixtures. The average rms difference for the CED results and for two group additivity predictive methods, Synthia–Fedors and Synthia–van Krevelen[20] with respect to the experimental values, is shown Table 5.

Solubility parameters predicted employing the current molecular dynamics simulation methodology can also be compared to those calculated employing molecular dynamics simulations by Rigby et al.[21a] Employing the PCFF force field and Amorphous Cell/Discover programs,[20] Rigby et al. predict solubility parameters for 13 of the molecules in Table 2, which have an rms difference with experiment of 0.92 $(cal/cm^3)^{1/2}$, which is similar to that predicted by the current methodology (rms difference of 1.1). As with the current simulations, the largest differences in the set are seen for two acid molecules. The current authors have calculated the solubility parameters for hexane, acetone, and *n*-propanol employing molecular dynamics simulations with the COMPASS force field and Amorphous Cell/Discover programs.[20] Average absolute differences with experiment for this set of three was found to be 0.25 with COMPASS methodology, smaller than the 0.55 difference observed for the current CED methodology. The COMPASS force field has been extensively optimized to reproduce heats of vaporization of a large number of organic liquids. For example, in a related COMPASS force field study,[21c] Sun has calculated heats of vaporization for 100 compounds to within an average percent error of experiment of −0.2% with maximum

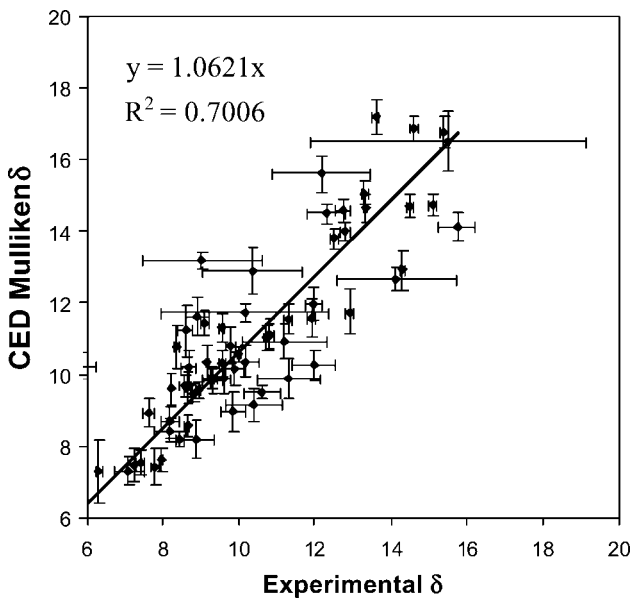

Figure 3. CED vs. experimental Hildebrand solubility parameters for all molecules in Table 2. Error bars indicate one experimental and simulation standard deviation. Charge assignment method is HF 6-31G** Mulliken population charges.

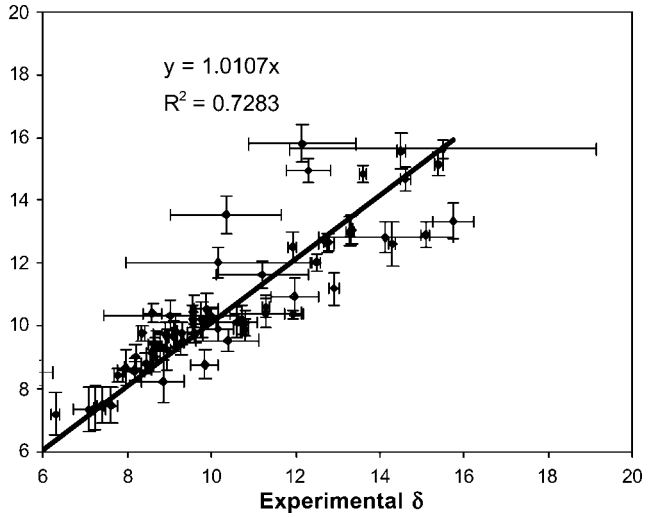

Figure 4. CED vs. experimental Hildebrand solubility parameters with quantum mechanical electrostatic potential (ESP) HF 6-31G** assigned charges. Error bars indicate one experimental and simulation standard deviation.

errors of 14.6 and 14.5%. This is to be contrasted with our current approach where generic force field was employed without any further optimization. Eichinger and coworkers[21b] have employed the COMPASS force field to compute solubility parameters for Ultem oligomers, related molecules, and solvent molecules including toluene. Not surprisingly, the calculated solubility parameter for toluene is 0.07 $(cal/cm^3)^{1/2}$ closer to the average experimental value [8.94 $(cal/cm^3)^{1/2}$] than the previous PCFF force field value.[21a] The calculated toluene solubility parameter value of 9.0

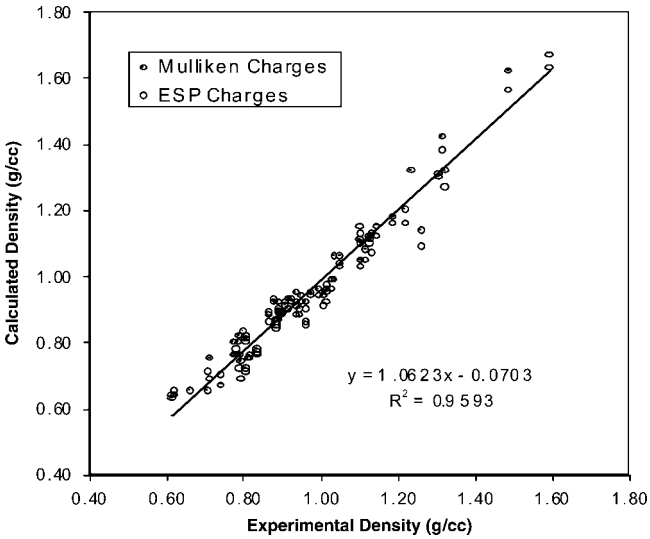

Figure 5. Calculated vs. experimental densities for 64 common solvents/monomers using the CED method. Deviations from experiment are 0.07 g/cc for either method.

Table 5. Average Error of Synthia Predictive Methods Compared with CED Predictions of Hildebrand Solubilities.

Method	RMS[a]
CED-ESP	1.17
Synthia-Fedor	1.388
Synthia-van-Krevelen	1.202

[a]Root-mean-square deviation (hildebrands).

$(cal/cm^3)^{1/2}$ compares well to the current ESP calculated solubility parameter of 9.23 $(cal/cm^3)^{1/2}$.

Electronic Nose Model

An electronic nose has been built at Caltech[22,23] employing an array of polymer sensors. Sensors are built with conducting leads connected through thin film polymers loaded with carbon black. Odorant detection relies on a change in electric resistivity, $\Delta R/R$, of the polymer film as a function of the amount of swelling caused by the odorant compound. The amount of swelling depends upon the chemical composition of the polymer and the odorant molecule. An array of 20 carbon black loaded polymers give rise to a specific change in resistivity patterns upon exposure to a given molecular species. The pattern is unique and unambiguously identifies the compound.[3,23]

The experimentally determined changes in relative resistivity, $\Delta R/R$, of seven polymer sensors upon exposure to 24 solvent vapors were correlated with the calculated Hansen solubility components. The permeability of a given odorant in a polymer is given by[24]

$$P = A \exp\left(\frac{\Delta H_s}{k_B T} - \frac{E_D}{k_B T}\right) \tag{5}$$

where A is the preexponential factor related to entropy, ΔH_s is the heat of sorption of the solute, and E_D is the activation energy for diffusion of the molecule in the polymer. We assume that the relative change in resistivity is directly proportional to the odorant's permeability. The following expression was used to correlate $\Delta R/R$ with the Hansen components of the cohesive energy of the polymer and solvent as well as the molar volume of the solvent[25]

$$\Delta R/R = R_o \exp(-\gamma V_s) \exp\left[\sum_{i=1}^{3} \beta_i (\delta_i^s - \delta_i^p)\right] \tag{6}$$

where γV_s is the activation energy of diffusion of the solute in the polymer, proportional to the molar volume of the odorant, V_s. The exponential factor γ is a best-fit parameter. We base this relation on the experimental observation that the diffusion coefficients of various molecules is linearly related to the molar volume of the solute in the case where the actual temperature is greater than the glass transition (T_g) of the polymer.[26] This approximation is used in our analysis regardless of T_g. δ_i^s (i = 1,2,3) are the cohesive

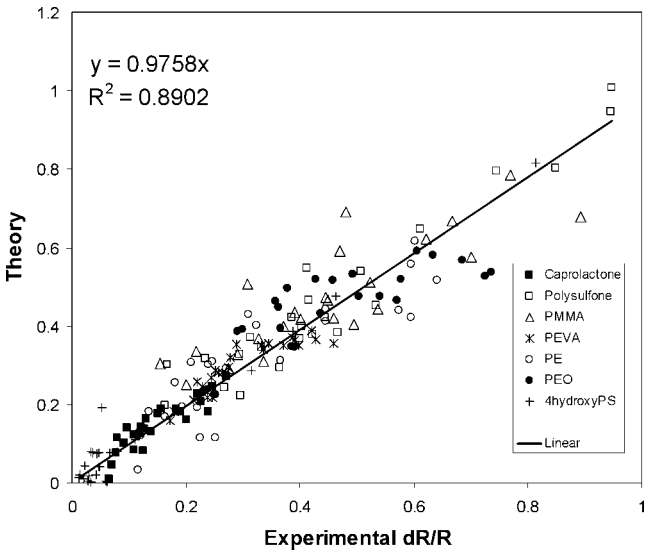

Figure 6. Comparison between theory, eq. (6), and experimental changes in resistivity of seven polymer sensors exposed to 24 solvents.

energy density component of the solvent s, where $i = 1$, 2, and 3 refer to the electrostatic, dispersion, and hydrogen bond components, respectively. Similarly, δ_i^p is the ith cohesive energy component of the polymer sensor p. The exponential coefficients β are treated as best-fit parameters as well as is the preexponential term R_0. It should be noted that we preserve the sign of the energy components in eq. (4), usually lost in the definition of Hansen and Hildebrand parameters. This is important because such interactions can be attractive or repulsive, depending on the polymer/odorant mixture in question.

The results of fitting eq. (6) to experimental changes in resistivity[27] are shown in Figure 6 for seven electronic nose polymer sensors and 24 solvents.[3,22] Pearson's correlations between the experimentally determined change in resistivity and the Hansen solubilities are shown for polymer sensors [poly(methylmethacrylate] (PMMA), poly(4-hydroxystyrene) (P4HS), polyethyleneoxide (PEO), polyethylene (PE), poly(ethylenevinyl acetate) (PEVA), polysulfone, and caprolactone) in Table 6. The calculated Hansen solubilities for the seven polymers and 24 solvents are summarized in Table 7. Note that in these calculations we used the generic Dreiding force field and the charge equilibration, Qeq,[14] method to assign atomic charges to polymers and solvent molecules. For more accurate results we recommend the use of quantum charges (ESP or Mulliken).

Table 6. Pearson's Correlation Coefficients and Slopes of Predicted vs Experimental Changes in Resistivity, $\Delta R/R$, for Each of Seven Polymer Vapor Solvent Detectors.

Polymer sensor	Slope	Pearson's R
Polycaprolactone	0.858	0.925
Polysulfone	0.932	0.962
PMMA	0.678	0.827
PEVA	0.888	0.936
Polyethylene	0.870	0.933
Polyethyleneoxide	0.746	0.874
Poly(4-hydroxystyrene)	1.018	0.991

Table 7. Calculated Cohesive Energy Density Components for Common Vapors and Polymers Employed in the Electronic Nose Design Work.

Odorants	ΔH_{vap} cal/cc	Electrostatic cal/cc	Dispersion cal/cc	H-bonding cal/cc
2-Pentanol	−151.42	−53.32	−76.48	−21.62
3-Pentanol	−142.40	−47.89	−76.87	−17.64
Amylacetate	−127.31	−40.19	−87.13	0.00
Butylacetate	−132.03	−41.75	−90.28	0.00
Decylacetate	−104.70	−21.02	−83.68	0.00
Ethanol	−257.64	−146.00	−51.35	−60.29
Ethylacetate	−159.31	−68.99	−90.33	0.00
Hexylacetate	−122.55	−34.83	−87.72	0.00
Iso-amylalcohol	−159.46	−59.82	−73.87	−25.77
Isoamylacetate	−125.90	−38.67	−87.24	0.00
Isoamylbenzoate	−119.56	−23.04	−96.52	0.00
Isoamylbutyrate	−111.52	−25.34	−86.17	0.00
Isoamylcaproate	−104.57	−20.83	−83.74	0.00
Isoamylpropionate	−113.17	−30.36	−82.81	0.00
Isobutylacetate	−130.92	−45.05	−85.87	0.00
Isopropylacetate	−143.46	−57.20	−86.26	0.00
n-Amylalcohol	−159.42	−59.53	−75.46	−24.44
n-Heptanol	−130.23	−37.63	−76.59	−16.01
n-Hexanol	−141.38	−46.42	−77.97	−16.99
n-Propanol	−193.82	−94.68	−60.77	−38.37
Octanol	−127.59	−33.80	−79.91	−13.88
Octylacetate	−112.37	−26.42	−85.95	0.00
Propylacetate	−142.96	−54.90	−88.06	0.00
n-Butanol	−152.72	−64.31	−61.58	−26.82
Polymer Sensor				
PMMA	−90.51	−31.19	−59.32	0.00
P4HS	−106.66	−28.66	−64.48	−13.51
PEO	−168.10	−68.36	−95.90	−3.84
PE	−85.45	−1.00	−84.46	0.00
PEVA	−85.02	−10.82	−74.20	0.00
Polysulfone	−138.74	−29.76	−108.98	0.00
Caprolactone	−122.66	−35.31	−87.34	0.00

The correlation was particularly good for polysulfone, poly(4-hydroxystyrene) and PEVA (polyethylene-*co*-vinyl acetate), and especially poor for polymethylmethacrylate based on both correlation slope and the Pearson R values for the linear fit. Polysulfone appears to discriminate between solvents of different sizes because the free volume fraction is small and the free volume distribution may be narrow, resulting in a "molecular sieve" effect. Additionally, the experimental relative change in resistivity in polysulfone ranges from zero to 1.0, which makes it a particularly good high-resolution sensor.

The polyethylene-*co*-vinyl acetate detector also correlates reasonably well with the theoretical relative change in resistivity. However, the relative change in resistivity range is smaller compared to polysulfone, indicating that it is less discriminating to-

wards ester and alcohol solvents. A possible explanation that accounts for this observation is that PEVA contains polar ester functional groups due to the vinyl content (18%), as well as nonpolar components due to the polyethylene content (82%). PEVA has a glass transition below room temperature, and as a result, contains a large free volume fraction. This decreases the sensitivity towards molecules of different sizes compared to high T_g polymers such as polysulfone. The third particularly good detector in terms of signal correlation with theoretical prediction is poly(4-hydroxy styrene). This detector is particularly sensitive to molecules functionalized with highly polar groups such as alcohol due to the hydroxyl functional group. However, the sensitivity of this sensor to moderately polar or nonpolar solvents such as esters is particularly low.

Conclusions

Hildebrand and Hansen solubility parameters play an important role in the development of stable commercial chemical formulations as well as for assessing phase segregation during product synthesis. Although various techniques are available to measure Hildebrand and Hansen solubility parameters, the experimental uncertainty in these measurements is significant for a large number of systems, particularly polymers and high boiling point substances. The CED method, a computational method, presented here offers consistent Hildebrand and Hansen solubility values over a large number of organic compounds of interest in formulation work. The use of multiple sampling techniques allows for the precise determination (ca. $\delta = 0.4$ hildebrands) of solubility parameters in a systematic way comparable to the experimental precision ($\delta = 0.43$). When combined with a generic force field and quantum mechanically determined atomic charges, CED yields first-principles hildebrand parameter predictions in good agreement with experiment (rms ca. 1.17 hildebrands). Accuracy is somewhat lower than precision probably due to the generic nature of the force field. No attempt was made to refine the force field parameters to improve the accuracy of the method, although such a possibility is clearly present.

We investigated the use of compression and expansion cycles, simulated annealing, charge assignment methods, and statistical sample averaging. It is important to start from a low-density sample to achieve equilibrated conformational statistics within a reasonable computational time. Ten samples, with roughly 1000 atoms each, seem surprisingly adequate to estimate these properties.

As parallel molecular dynamics algorithms are implemented, simulation times will be reduced and the prediction of solubility parameters will become even more practical. For example, the estimation of Hildebrand and Hansen solubility parameters takes approximately 2 h in a dual processor Linux computer. Using a highly parallel particle-mesh algorithm[28,29] to integrate the dynamics, the CPU times can be reduced to a few minutes using 24 processors. In such a computational environment, it becomes practical to automate the population of databases of solvents and complex mixtures with Hildebrand and Hansen solubility parameters for product formulation work. Simulation times are short enough to allow the batch development of computer generated material/solvent databases.

Finally, the CED method provides a simple protocol that overcomes the common equilibration problems with condensed phase molecular dynamics, that is, how to choose initial molecular configurations not far from equilibrium at normal bulk densities. We applied the method to the problem of predicting responses of polymeric sensors in an electronic nose to the presence of vapor compounds. The models Person's coefficients range from 0.82 to 0.99, depending on the polymer sensor. Other practical uses include the selection of polymers in blends, solvents, and additives in chemical, cosmetic, and pharmaceutical formulations, and the design of chemical synthesis processes.

Acknowledgments

The authors would like to thank Prof. Nathan S. Lewis and postdoctoral fellow Glen Walker for generously providing experimental polymer sensor data for the electronic nose prior to publication. The facilities of the MSC were partly funded by NSF MRI, and ARO/DURIP, and are also supported by grants from DOE-ASCI, Chevron, NIH, ONR, Seiko-Epson, Avery-Dennison, Kellogg's, General Motors, Beckman Institute, Asahi Chemical, and Nippon Steel.

References

1. Hildebrand, J. H. The Solubility of Non-Electrolytes; New York: Reinhold, 1936.
2. Hansen, C. M. J Paint Technol 1967, 39, 511.
3. Severin, E. J.; Doleman, B. J.; Lewis, N. S. Anal Chem 2000, 72, 658.
4. Choi, P.; Kavassalis, T. A.; Rudin, A. J Colloid Interface Sci 1992, 150, 386.
5. Kavassalis, T. A.; Choi, P.; Rudin, A. Mol Simul 1993, 11, 229.
6. Rogel, E. Energy Fuels, 1997, 11, 920.
7. Kotelyanskii, M. Trends Polym Sci 1997, 5, 192.
8. Khare, R.; Paulaitis, M. E.; Lustig, S. R. Macromolecules 1993, 26, 7203.
9. Rapold, R. F.; Suter, U. W.; Theodorou, D. N. Macromol Theory Simul 1994, 3, 19.
10. Roe, R. J.; Rigby, D. J Phys Chem 1998, 89, 5280.
11. Furuya, H.; Mondello, M.; Yang, H. J.; Roe, R. J. Macromolecules 1994, 27, 5674.
12. Roe, R. J. Computer Simulation of Polymers; Roe, R. J., Ed.; Polymer Science and Engineering, Prentice-Hall: Englewood Cliffs, NJ, 1991.
13. Gusev, A. A.; Zender, M. M.; Suter, U. W. Macromolecules, 1994, 27, 615.
14. Rappe, A. K.; Goddard, W. A., III. J Phys Chem 1991, 95, 3358.
15. (a) van Krevelen, D. W. Properties of Polymers: Their Correlation with Chemical Structure; Their Numerical Estimation and Prediction from Group Contributions; Elsevier Science Publishers: New York, 1990, p. 536; (b) Ibid, p. 575.
16. Mayo, S. L.; Olafson, B. D.; Goddard, W. A., III. J Phys Chem 1990, 94, 8897.
17. Originally part of the suite of programs in Polygraf, the amorphous builder is part of the Cerius2 software package, Cerius2, Accelrys, Inc., San Diego, CA.

18. Rappé, A. K.; Casewit, C. J.; Colwell, K. S. ; Goddard, W. A., III; Skiff, W. M. J Am Chem Soc 1992, 114, 10024.
19. Box, G. E. P.; Hunter, W. G.; Hunter, J. S. Statistics for Experimenters, An Introduction to Design, Data Analysis, and Model Building; John Wiley & Sons: New York, 1978.
20. (a) Computational results obtained using software programs from Accelrys, Inc. San Diego, CA. Property/structure solubility parameters calculated employing Synthia program. Molecular dynamics results obtained employing the COMPASS force field with Amorphous Cell/Discover Programs; (b) MDL® Polymer, San Leandro, CA; (c) Van Krevelen, D. W. Properties of Polymers; Elsevier: New York, 1990; (d) Bicerano, J. Prediction of Polymer Properties; Macel Decker Inc.: New York, 1993.
21. (a) Eichinger, B. E.; Rigby, D. R.; Muir, M. H. Comp Polym Sci 1995, 5, 147; (b) Eichinger, B. E.; Rigby, D. R.; Stein, J. Polymer 2002, 43, 5999; (c) Sun, H. J Phys Chem B 1998, 102, 7338.
22. G. Walker, N. Lewis, private communication.
23. Lonergan, M. C.; Severin, E. J.; Doleman, B. J.; Beaber, S. A.; Grubb, R. H.; Lewis, N. S. Chem Mater 1996, 8, 2298.
24. Weast, R.C.; Astle, M. J. CRC Handbook of Chemistry and Physics; CRC Press: Boca Raton, FL, 1980, p. 732, 60th ed.
25. (a) Belmares, M. P. Ph.D. Caltech Thesis, UM #9916173, 1998; (b) The procedure has been coded as a single application using the Software Developer's Kit (SDK) in Cerius2, Accelrys, Inc., San Diego, CA.
26. van Krevelen, D. W. Properties of Polymers: Their Correlation with Chemical Structure; Their Numerical Estimation and Prediction from Group Contributions; Elsevier Science Publishers: New York, 1990.
27. Severin, E. J. Caltech Dissertation, 1999.
28. Plimpton, S. J.; Pollock, R.; Stevens, M. Proc of the Eighth SIAM Conference on Parallel Processing for Scientific Computing, Minneapolis, MN, March, 1997.
29. Plimpton, S. J. J Comp Phys., 1995, 117, 1.
30. Gordon, J.; Giauque, W. F. J Am Chem Soc 1948, 70, 1506.
31. Hoy, K. L. J Paint Technol 1970, 42, 79.
32. Brandrup, J.; Immergut, E. H.; Grulke, E. A., Eds. Polymer Handbook; Wiley: New York, 1999, 4th ed.
33. Barton, A. F. M., Ed. CRC Handbook of Solubility Parameters and Other Cohesion Parameters; CRC Press: Boca Raton, FL, 1991, p. 94, 153, 4th ed.
34. Rodriguez, F., Ed. Principles of Polymer Systems; McGraw-Hill: New York, 1982, p. 25, 2nd ed.
35. Askadskii, A. Physical Properties of Polymers—Prediction and Control; Gordon and Breach: Amsterdam, 1996, p. 41.
36. Teas, J. The Journal of Paint Technology 1968, 40, 19.
37. Newman, S. In Polymer Blends; Paul, D. R., Ed.; Academic Press, Inc.: Orlando, 1978, vol. 1.